

Figure 1. Dynamics of the Polar Cap Movement

(A) Gic2p₍₁₋₂₀₈₎-GFP is used as a reporter for activated Cdc42p. Localized fluorescence signal in wild-type (strain ERT224.1; upper panel) or *rsr1Δ* (strain ERT225.1; lower panel) cells. Time is reported in minutes.
 (B) Bem1p-CFP localization is shown in an *rsr1Δ* (strain ERT273.2) cell. Time is reported in minutes.
 (C) Time evolution of the polarization angle in a wild-type (open circles) or *rsr1Δ* (solid red circles) cell. The polarization angle is defined as the angle difference between the current and incipient polarization site.

after the initial establishment of cellular polarity, although the cap displayed small displacements. Eventually, budding started adjacent to the previous division site (Figure 1A, upper panel; Movie S1). Similar behavior was observed in *bem1Δ* cells. This is expected because in these cells the budding landmark is fully functional and cells bud in a nonrandom, monopolar fashion.

If dynamic polarization in the absence of landmark protein Rsr1p (Bud1p) is solely determined by autoamplification of fluctuations in Cdc42p regulators, we expected that a polar cap would be initiated at a random location followed by budding at this same location. Indeed, the polar cap formed at a single site, but contrary to the above expectations, it started to move around the cell periphery immediately after symmetry breaking. The direction of movement changed at random time intervals. Occasionally, polar caps traveled over the entire cell perimeter before settling down at a random location to initiate budding (Figure 1A, lower panel; Movies S2 and S3). Similar behavior was observed when the location of the polar cap components was monitored by Bem1p-CFP (Figure 1B), Gic2p-GFP, and CRIB_{Cla4}-GFP (data not shown). The interval between the appearance of the polar cap and the inception of budding at room temperature is (60 ± 13) min (N = 13). We find that the wandering stops about 15–20 min before we can detect the appearance of the bud in the phase contrast image. The motion of traveling polar caps was quantified by their angular displacement with respect to the initial polarization site at the start of the experiment. Analysis of the polarization angle indicates that there is a significant difference in mobility of the polar caps between wild-type and *rsr1Δ* cells over the entire G1 stage of the cell cycle (Figure 1C).

The mobility of the traveling activity waves was quantified by plotting the mean square angular displacement of polar caps θ_{RMS}^2 as a function of time, averaged over multiple cells (Saxton and Jacobson, 1997). The linear dependence of θ_{RMS}^2 with time for *rsr1Δ* cells re-

veals that traveling waves perform a random unconstrained walk at the cell periphery (Figure 2A). Deletion of other landmark proteins, such as Bud2p and Bud5p, also resulted in the appearance of traveling waves. The mobility of the polar caps as measured by the slope of the θ_{RMS}^2 -time relation showed similar values for *rsr1Δ*, *bud2Δ*, and *bud5Δ* cells (Figure 3A). This indicates that cycling between the GTP and GDP-bound state of Rsr1p is necessary to prevent the polar cap from traveling, because cells expressing constitutively active and inactive Rsr1p (*bud2Δ* and *bud5Δ* cells, respectively) display highly mobile waves.

Dosage Dependence of Wave Mobility on Localizing Factors

The above results suggest the existence of pattern-destabilizing processes, which become dominant in the absence of localizing factors such as Rsr1p. Next, we reduced the Rsr1p expression level below the wild-type level to attain an intermediate level of polarizing strength and to moderate the effect of pattern destabilization. For this purpose, the weak P_{IXR1} and P_{GLN3} promoters (Holland, 2002) were used to drive to expression of *RSR1*. The mobility of the polar cap was reduced in comparison to *rsr1Δ* cells as the concentration of Rsr1p increased (Figure 2A). When *RSR1* is driven by the weak P_{GLN3} promoter, the increase of θ_{RMS}^2 slowed down with time, indicative of confined random motion of the polar cap (Saxton and Jacobson, 1997). This is consistent with the model that large fluctuations in pattern destabilization cause the polar cap to escape from the area of activated Rsr1p localization at low expression level. However, on average, the polar cap spends more time in the area of landmark proteins. In order to examine how the wave mobility affects bud site selection, we measured the budding angle. The budding angle reflects the displacement of the settled, late G1 localization of the polar cap with respect to the previous budding site (see Experimental Procedures). The average budding angle correlates nonlinearly with the wave mo-

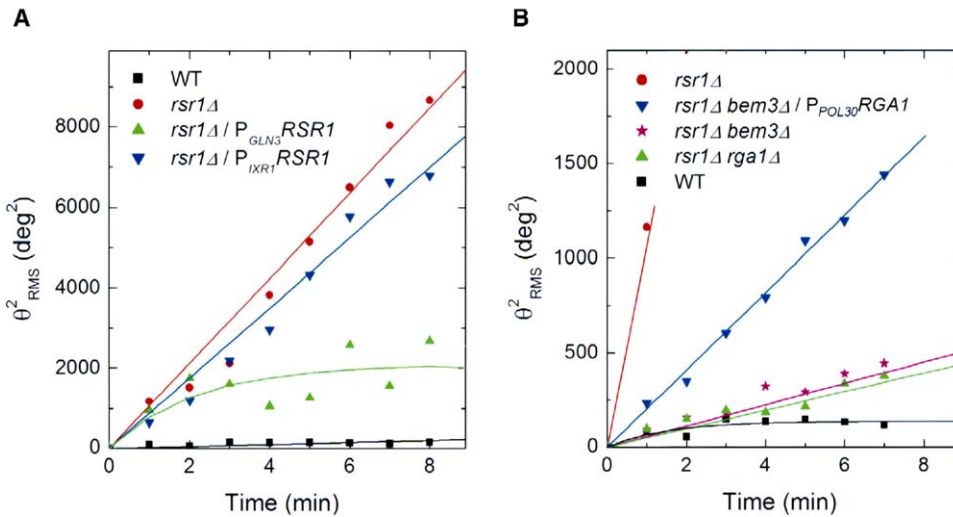


Figure 2. The Root Mean Square of the Angular Displacement θ_{RMS}^2 of the Polar Cap Quantifies Wave Mobility

θ_{RMS}^2 is plotted as a function of time with respect to the initial polarization angle at the start of the observation. θ_{RMS}^2 was obtained by averaging over at least ten different cells. The average slope, obtained by a linear least-square fit, of θ_{RMS}^2 -time relation defines the wave mobility.

(A) Dosage-dependent effect of *RSR1* expression on the motility of the polar cap shown for wild-type (strain ERT224.1; black squares), *rsr1* Δ (strain ERT225.1; red circles), *rsr1* Δ /*P*_{GLN3}*RSR1* (strain ERT275.2; green triangles), and *rsr1* Δ /*P*_{IXR1}*RSR1* (strain ERT276.3; green triangles) cells.

(B) Dosage-dependent effect of GAP expression on the motility of the polar cap for wild-type (strain ERT224.1; black squares), *rsr1* Δ (strain ERT225.1; red circles), *rsr1* Δ *bem3* Δ /*P*_{POL30}*RGA1* (strain ERT282.3; blue triangles), *rsr1* Δ *bem3* Δ (strain ERT254.1; purple stars), and *rsr1* Δ *rga1* Δ (strain ERT255.1; green triangles) cells.

bility (Figure 3B), revealing that confinement of waves results in a more deterministic bud site selection.

Regulators of Cdc42p GTPase Activity Determine the Mobility of Waves

Whereas landmark proteins localize the traveling waves, activities that enhance the mobility of the waves are likely to be related to restructuring of the polar cap. Cycling of Cdc42p between GTP and GDP-bound forms is crucial for recruitment of polar cap components (Irazoqui et al., 2003, 2004). Inhomogeneous recruitment of Cdc42p regulators within the polar cap may lead to a local decrease in the Cdc42p turnover and, consequently, the net dissociation rate of polar cap components would increase. As a result, the restructuring and mobility of the polar cap would be reduced. The spatial distribution of Cdc42p and its regulators bound to secretory or endocytotic vesicles is in part dependent on actin-based transport (Wedlich-Soldner et al., 2004; Irazoqui et al., 2005). Therefore, we hypothesized that impairment of actin polymerization or changing the turnover of the Cdc42p GTPase cycle would decrease the wave mobility. First, inhibition of actin polymerization by latrunculin A abolished wave mobility in *rsr1* Δ cells (Figure 3A). While initial pattern formation is independent of actin even in the absence of landmark proteins (Ayscough et al., 1997; Irazoqui et al., 2003; Figure S2), the mobility and the dynamic nature of polar caps is actin-dependent. The wave mobility in latrunculin A-treated *rsr1* Δ cells is very similar to that observed for wild-type cells. We do not observe the alternating appearance and disappearance of the polar cap as was observed

when Cdc42p-GFP was used as a reporter in latrunculin A-treated cells (Wedlich-Soldner et al., 2004). This difference might be attributed to use of a different reporter or different expression levels of Cdc42p or Rsr1p in these strains. Second, the turnover of the Cdc42p GTPase cycle was impaired by deleting *BEM3*, a gene encoding a GAP protein for Cdc42p. This deletion reduced the wave mobility substantially in *rsr1* Δ cells (Figures 2B and 3A). To verify whether this phenotype was specific to the deletion of *BEM3* or whether it reflects the reduction of GAP activity in general, another GAP gene, *RGA1*, was deleted. The effect of this deletion was comparable to that observed for the *BEM3* deletion. In addition, overexpression of Rga1p in *rsr1* Δ *bem3* Δ cells restored the mobility of the polar cap (Figures 2B and 3A). When *BEM3* is overexpressed in *rsr1* Δ cells, the wave mobility does not change appreciably, indicating that the wave mobility in *rsr1* Δ cells is close to its maximum saturated value (Figure 3A). This might indicate that there is another limiting factor that determines the maximum recruitment rate of the GAPs to the polarization site. These data suggest that wave mobility depends on the dosage of GAP activity. Third, overexpression of a cell membrane-targeted form of the GEF Cdc24p also resulted in a decreased mobility (Figure 3A) of a more widely distributed polar cap (Supplemental Data).

A Model of Feedback Regulation of Cdc42p Activity Explains Wave Formation

The formation of Cdc42p activity waves can be modeled in terms of a feedback control of activators and

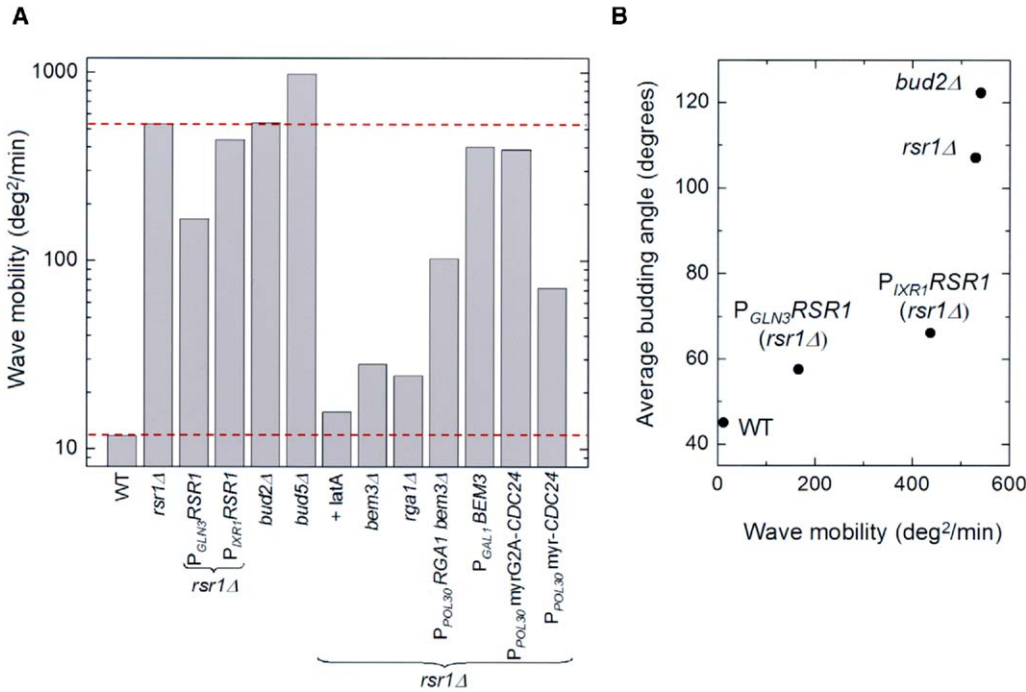


Figure 3. Regulation of Wave Mobility and Effect on the Budding Angle

(A) Wave mobility (units of deg²/min) of the polar cap in cells having different genetic backgrounds. The same strains were used as described in Figure 2. The last two bars were obtained from cells overexpressing myrG2A-CDC24 (strain ERT236.1) and myr-CDC24 (strain ERT237.1). (B) The wave mobility nonlinearly correlates with the average budding angle of cells expressing varying amounts of landmark proteins. In wild-type cells, new buds are excluded from the previous budding sites. This results in a minimum budding angle of around 40° for wild-type cells. An angle of about 120° corresponds to random budding.

inhibitors of Cdc42p (Figure 4A; Supplemental Data). Interactions between Bem1p, Cdc24p, and Cdc42p are suggested to form an actin-independent, positive feedback loop that enhances the recruitment of activators to the polar cap (Bose et al., 2001; Butty et al., 2002; Irazoqui et al., 2003; Wedlich-Soldner et al., 2003, 2004; Shimada et al., 2004). We hypothesize that this positive feedback loop accounts for the initial symmetry breaking (Figure S2). A second, actin-mediated, positive feedback could be mediated by the actin-based delivery of secretory vesicles containing, for example, Cdc42p or Cdc24p (Wedlich-Soldner et al., 2003, 2004). Indeed, we sometimes observe faint Gic2p₁₋₂₀₈-GFP-labeled dots moving toward the polar cap (Figure S4).

Positive feedback loops allow an initially homogeneous system to polarize in a random static direction (Gierer and Meinhardt, 1972). Because there is a limited number of activated Cdc42p molecules distributed along the membrane, a uniform distribution will still exhibit small local concentration deviations about the average. Due to the positive feedback regulation, local concentration maximums will grow at the expense of the surrounding areas in the membrane. This mechanism can explain the initial symmetry breaking in, for example, latrunculin-treated cells (Figure 4B, middle panel), but cannot explain the traveling Cdc42p activity waves.

We therefore propose that in addition to the positive regulation, a negative feedback loop must exist. Be-

cause we do not observe waves in latrunculin-treated cells, it is likely that the negative feedback loop is mediated by the actin cytoskeleton. A potential molecular implementation of the negative loop might be the delivery of vesicles containing GAPs along the actin cables. Alternatively, recent experiments show that actin-dependent endocytosis might disperse polarizing factors (Irazoqui et al., 2005). Because actin patch components (associated with endocytosis) can be recruited by Cdc42p-GTP (Lechler et al., 2000), this indicates that Cdc42p could stimulate dispersal of polarized factors in an actin-dependent manner, effectively establishing a negative feedback loop. The negative feedback loop provides the system with the potential to exhibit traveling waves (Meinhardt, 1999). To observe traveling waves, it is important that the negative feedback regulation operates at a slower rate than the positive regulation. We propose that the actin-independent positive feedback reacts faster to a change in Cdc42p activation state than the regulation mediated by the actin cytoskeleton. This is a reasonable assumption because nucleation and polymerization of new actin cables followed by vesicle transport might be a slower process than the formation of the Bem1p scaffolding complex that relies on relatively fast protein-protein interactions and rapid diffusion. We propose that the waves observed in *rsr1Δ* cells are a result of a competition between a fast, actin-independent, positive feedback regulation and a slow and therefore delayed, negative feedback regulation.

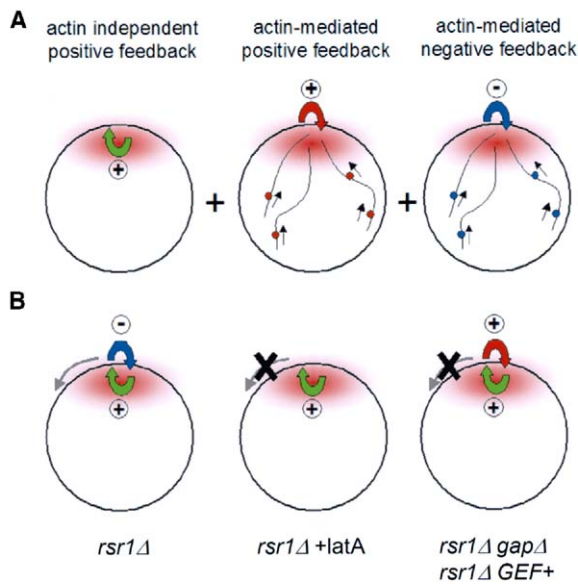


Figure 4. Hypothetical Model of Wave Formation of Cdc42p Regulators

(A) Three feedback loops regulate the recruitment of Cdc42p regulators: an actin-independent positive feedback loop (left), an actin-mediated positive feedback loop (middle), and an actin-mediated negative feedback loop (right).

(B) Initiation of waves (indicated by gray arrow) is expected in cells for which the actin-mediated negative feedback dominates the actin-mediated positive feedback (left). This net negative feedback can destabilize the polar cap and initiate cap motion. No wave mobility is expected when the positive feedback loops dominate. This can be achieved in the absence of the actin cytoskeleton (+lata, middle) or in strains in which the GAP activity is reduced or the Cdc42p activity is enhanced (*gap*Δ or *GEF*+, right). More details on the model are given in Supplemental Data.

Because the inactivation always lags behind the spreading activation, this induces a wave motion (Meinhardt, 1999). This implies that in *rsr1*Δ cells, the actin-mediated negative feedback dominates the actin-mediated positive feedback. Wandering of the polar cap was not observed in earlier experiments in which the position of the polar cap was monitored by using a GFP fusion of wild-type Cdc42p or a constitutively activated version of Cdc42p (Wedlich-Soldner et al., 2003, 2004). The strains used in these experiments carried a functional *RSR1* gene and expressed higher levels of activated Cdc42p compared to wild-type. This elevated Cdc42p activity leads to a stronger actin-mediated positive feedback, which might explain the absence of Cdc42p activity waves in these strains.

In *rsr1*Δ cells, the effective feedback systems consist of one actin-independent positive feedback and one actin-mediated negative feedback (Figure 4B, left panel). The opposite holds for *rsr1*Δ cells in which the GAP activity has been reduced or the GEF activity has been increased. In these cells, the positive, actin-mediated loop dominates the negative feedback and therefore the feedback structure consists effectively of two parallel positive loops that allow symmetry breaking but do not support wave mobility (Figure 4B, right panel). In

the absence of the cytoskeleton, only one positive feedback loop remains, explaining the absence of waves in latrunculin-treated cells (Figure 4B, middle panel). The proposed feedback system (Figure 4A) therefore qualitatively explains all the experimental data. A numerical model that explicitly models the dynamics in the different mutants is presented in Supplemental Data. The above model is likely to account for cellular polarization in other contexts, for example during cell shape changes upon exposure of yeast cells to pheromones. Interestingly, wandering polar caps were also observed in pheromone-treated mutant strains that lack landmark proteins and are defective in chemotaxis (Nern and Arkowitz, 2000).

Conclusion

Cdc42 is essential for chemotaxis in higher eukaryotes such as *Dictyostelium* and neutrophils (Watanabe et al., 2004; Weiner et al., 2002). In these cells, interlocked positive and negative feedback loops have been identified among Cdc42, its regulators, and the actin network (Meili and Firtel, 2003). Similar arguments that explain the Cdc42p activity waves in budding yeast might apply to the rotating pseudopod waves observed in *Dictyostelium* (Killich et al., 1993, 1994) or the minCDE oscillatory waves in *Escherichia coli* (Meinhardt and de Boer, 2001; Huang et al., 2003). Mechanisms responsible for symmetry breaking are inherently coupled to mechanisms that enable restructuring of patterns. A design of competing feedback regulation loops combines efficient polarization with the ability to dynamically respond to varying intracellular or environmental conditions.

Experimental Procedures

Construction of Plasmids and Strains

The P_{GLN3} , P_{IXR1} , P_{MYO2} , and P_{POL30} promoter sequences correspond to the 600, 858, 677, and 600 base pair regions upstream of the start codon of the respective genes. P_{TET02} corresponds to the CYC1 TATA region with two upstream rTA binding sites. The T_{RSR1} , T_{CDC24} , and T_{CYC1} terminator sequences correspond to the 596, 373, and 204(187) base pair regions downstream of the stop codon of the respective genes. BamHI-RGA1 (1–60 stop codon)-NotI fragment was cloned into pRS401 backbone downstream of P_{POL30} . A sequence encoding the MGCTVSTQTIGDESDP myristoylation signal or a mutated signal sequence (G2A) was fused to the N terminus of *CDC24* by PCR. The resulting BamHI-myr-*CDC24*- T_{CDC24} -NotI and BamHI-myr(G2A)-*CDC24*- T_{CDC24} -NotI constructs were cloned into pRS316 and pRS401 backbones downstream of P_{POL30} . KpnI- P_{MYO2} -rTA- T_{CYC1} -NotI was cloned into pRS305 and pRS401 backbones. KpnI- P_{GLN3} -*RSR1*- T_{RSR1} -NotI and KpnI- P_{IXR1} -*RSR1*- T_{RSR1} -NotI was cloned into pRS401 backbone. XhoI- P_{TET02} -(BamHI/BglII)-GIC2(1–208)-(BglII/BamHI)-GFP- T_{CYC1} -NotI was cloned into pRS306 backbone. All strains are derivatives of BY4741 (MATA *his3*Δ1 *leu2*Δ0 *met15*Δ0 *ura3*Δ0). The strain list is given in Table S1. Plasmid MJ792 was a gift from M. Peter.

Growth Conditions and Data Acquisition

Yeast cells were grown overnight at 30°C in synthetic selective dextrose media. Expression of GIC2(1–208)GFP was induced overnight by doxycycline addition (50 μg/l) into the growth media. Cells were harvested at exponential growth. For time-lapse experiments, slides were covered with 1% agarose containing synthetic media supplemented with 2% glucose. Cells were spun down and resuspended in the same media and placed on top of a thin agar layer. Fluorescence signals of single cells were measured using a Nikon

TE2000 microscope (Microvideo Instruments, Avon, MA) with automated stage and a cooled back-thinned CCD camera (Micromax; Roper Scientific, Duluth, GA). Imaging was performed at room temperature ($T = 22^{\circ}\text{C}$). Images were collected every 60 s to follow the movement of the polar cap. The site of maximum fluorescence intensity in the polar cap was marked as the center of the cap. The angle between the initial and subsequent centers of the moving polar cap was calculated using Metamorph (Universal Imaging; Research Precision Instruments, Natick, MA). On average, 30 time series were obtained to calculate the θ_{RMS} in each genetic background. The wave mobility was calculated from fitting the θ_{RMS}^2 time plot between $t = 0$ and 10 min using a linear least square fit. Cells in the G1 stage had polar caps wandering around the cell periphery which stopped around 15–20 min before the onset of budding (S phase). In addition, a small fraction of cells in G1 stage (<20%) had polar caps which either did not move or the movement paused for a longer time period (around 20–25 min). Some of these cells did not bud at all, which may reflect that they entered a quiescent state. For calculating the mobility coefficients, cells were considered in which the polar caps did not stop or pause. For measuring the budding angle, cells were stained with ConA (Lew and Reed, 1993). The angle between a small bud and the birth scar in daughter and young mother cells was measured. Both *rsr1 Δ berm3 Δ* and *rsr1 Δ rga1 Δ* cells continued budding randomly like *rsr1 Δ* cells, as assayed by budding angle (data not shown), although the stability of the position of the polar cap in these cells was similar to that in wild-type cells. For actin depolymerization, cells were treated with 100 μM latrunculin A for 10 min. Cells suspended in media containing latrunculin A were placed on a thin agar layer and microscopy was performed as described above. For FRAP experiments, a small region in the middle of the polar cap was bleached and fluorescence recovery was followed by confocal microscopy.

Supplemental Data

Supplemental data including a computer simulation, discussion, figures, table, and movies are available at <http://www.developmentalcell.com/cgi/content/full/9/4/565/DC11>.

Acknowledgments

We thank J. Chabot for technical assistance, B. Tam for help with confocal microscopy, D. Pellman, J. Pedraza, and S. Oliferenko for helpful suggestions and critical reading of the manuscript, and M. Peter, D. Lew, E. Bi, and D. Pellman for kindly providing strains and plasmids. A.B. is a Long-Term Fellow of the Human Frontier Science Program. This work was supported by NSF-CAREER (PHY-0094181) and NIH (GM068957) grants.

Received: February 21, 2005

Revised: August 3, 2005

Accepted: August 29, 2005

Published: October 3, 2005

References

Ayscough, K.R., Stryker, J., Pokala, N., Sanders, M., Crews, P., and Drubin, D.G. (1997). High rates of actin filament turnover in budding yeast and roles for actin in establishment and maintenance of cell polarity revealed using the actin inhibitor latrunculin-A. *J. Cell Biol.* **137**, 399–416.

Bose, I., Irazoqui, J.E., Moskow, J.J., Bardes, E.S., Zyla, T.R., and Lew, D.J. (2001). Assembly of scaffold-mediated complexes containing Cdc42p, the exchange factor Cdc24p, and the effector Cla4p required for cell cycle-regulated phosphorylation of Cdc24p. *J. Biol. Chem.* **276**, 7176–7186.

Burbelo, P.D., Drechsel, D., and Hall, A. (1995). A conserved binding motif defines numerous candidate target proteins for both Cdc42 and Rac GTPases. *J. Biol. Chem.* **270**, 29071–29074.

Butty, A.C., Perrinjaquet, N., Petit, A., Jaquenoud, M., Segall, J.E., Hofmann, K., Zwahlen, C., and Peter, M. (2002). A positive feedback loop stabilizes the guanine-nucleotide exchange factor Cdc24 at sites of polarization. *EMBO J.* **21**, 1565–1576.

Caviston, J.P., Tcheperegine, S.E., and Bi, E. (2002). Singularity in budding: a role for the evolutionarily conserved small GTPase Cdc42p. *Proc. Natl. Acad. Sci. USA* **99**, 12185–12190.

Chant, J. (1999). Cell polarity in yeast. *Annu. Rev. Cell Dev. Biol.* **15**, 365–391.

Gierer, A., and Meinhardt, H. (1972). A theory of biological pattern formation. *Kybernetik* **12**, 30–39.

Holland, M.J. (2002). Transcript abundance in yeast varies over six orders of magnitude. *J. Biol. Chem.* **277**, 14363–14366.

Huang, K.C., Meir, Y., and Wingreen, N.S. (2003). Dynamic structures in *Escherichia coli*: spontaneous formation of MinE rings and MinD polar zones. *Proc. Natl. Acad. Sci. USA* **100**, 12724–12728.

Irazoqui, J.E., Gladfelter, A.S., and Lew, D.J. (2003). Scaffold-mediated symmetry breaking by Cdc42p. *Nat. Cell Biol.* **5**, 1062–1070.

Irazoqui, J.E., Gladfelter, A.S., and Lew, D.J. (2004). Cdc42p, GTP hydrolysis, and the cell's sense of direction. *Cell Cycle* **3**, 861–864.

Irazoqui, J.E., Howell, A.S., Theesfeld, C.L., and Lew, D.J. (2005). Opposing roles for actin in Cdc42p polarization. *Mol. Biol. Cell* **16**, 1296–1304.

Killich, T., Plath, P.J., Xiang, W., Bultmann, H., Rensing, L., and Vicker, M.G. (1993). The locomotion shape and pseudopodial dynamics of unstimulated *Dictyostelium* cells are not random. *J. Cell Sci.* **106**, 1005–1013.

Killich, T., Plath, P.J., Hass, E.C., Xiang, W., Bultmann, H., Rensing, L., and Vicker, M.G. (1994). Cell-movement and shape are nonrandom and determined by intracellular, oscillatory rotating waves in *Dictyostelium* amoebae. *Biosystems* **33**, 75–87.

Kozminski, K.G., Beven, L., Angerman, E., Tong, A.H., Boone, C., and Park, H.O. (2003). Interaction between a Ras and a Rho GTPase couples selection of a growth site to the development of cell polarity in yeast. *Mol. Biol. Cell* **14**, 4958–4970.

Lechler, T., Shevchenko, A., and Li, R. (2000). Direct involvement of yeast type I myosins in Cdc42-dependent actin polymerization. *J. Cell Biol.* **148**, 363–373.

Lew, D.J., and Reed, S.I. (1993). Morphogenesis in the yeast cell cycle: regulation by Cdc28 and cyclins. *J. Cell Biol.* **120**, 1305–1320.

Meili, R., and Firtel, R.A. (2003). Two poles and a compass. *Cell* **114**, 153–156.

Meinhardt, H. (1999). Orientation of chemotactic cells and growth cones: models and mechanisms. *J. Cell Sci.* **112**, 2867–2874.

Meinhardt, H., and de Boer, P.A.J. (2001). Pattern formation in *E. coli*: a model for the pole-to-pole oscillations of Min proteins and the localization of the division site. *Proc. Natl. Acad. Sci. USA* **98**, 14202–14207.

Nelson, W.J. (2003). Adaptation of core mechanisms to generate cell polarity. *Nature* **422**, 766–774.

Nern, A., and Arkowitz, R.A. (2000). G proteins mediate changes in cell shape by stabilizing the axis of polarity. *Mol. Cell* **5**, 853–864.

Park, H.O., Bi, E., Pringle, J.R., and Herskowitz, I. (1997). Two active states of the Ras-related Bud1/Rsr1 protein bind to different effectors to determine yeast cell polarity. *Proc. Natl. Acad. Sci. USA* **94**, 4463–4468.

Saxton, M.J., and Jacobson, K. (1997). Single-particle tracking: applications to membrane dynamics. *Annu. Rev. Biophys. Biomol. Struct.* **26**, 373–399.

Shimada, Y., Wiget, P., Gulli, M.P., Bi, E., and Peter, M. (2004). The nucleotide exchange factor Cdc24p may be regulated by auto-inhibition. *EMBO J.* **23**, 1051–1062.

Toenjes, K.A., Simpson, D., and Johnson, D.I. (2004). Separate membrane targeting and anchoring domains function in the localization of the *S. cerevisiae* Cdc24p guanine nucleotide exchange factor. *Curr. Genet.* **45**, 257–264.

Watanabe, T., Wang, S., Noritake, J., Sato, K., Fukata, M., Takefuji, M., Nakagawa, M., Izumi, N., Akiyama, T., and Kaibuchi, K. (2004). Interaction with IQGAP1 links APC to Rac1, Cdc42, and actin filaments during cell polarization and migration. *Dev. Cell* **7**, 871–883.

Wedlich-Soldner, R., Altschuler, S., Wu, L., and Li, R. (2003). Spontaneous cell polarization through actomyosin-based delivery of the Cdc42 GTPase. *Science* 299, 1231–1235.

Wedlich-Soldner, R., Wai, S.C., Schmidt, T., and Li, R. (2004). Robust cell polarity is a dynamic state established by coupling transport and GTPase signaling. *J. Cell Biol.* 166, 889–900.

Weiner, O.D., Neilsen, P.O., Prestwich, G.D., Kirschner, M.W., Cantley, L.C., and Bourne, H.R. (2002). A PtdInsP(3)- and Rho GTPase-mediated positive feedback loop regulates neutrophil polarity. *Nat. Cell Biol.* 4, 509–513.